JOURNAL OF GUIDANCE, CONTROL, AND DYNAMICS
Vol. 17, No. 3, May–June 1994

# Implementation of a Full-Envelope Controller for a High-Performance Aircraft

Richard J. Adams,* James M. Buffington,† and Siva S. Banda‡
*Wright Laboratory WL/FIGC, Wright-Patterson Air Force Base, Ohio 45433*

**The design, implementation, and evaluation of a full-envelope control system for the AIAA controls design challenge aircraft is presented. The control problem is divided into separate longitudinal and lateral/directional designs. The longitudinal controller is a Mach number and flight path angle command system, and bank angle is commanded through the lateral/directional autopilot. A cross-axis filter minimizes transient errors during coupled maneuvers. Proportional plus integral plus derivative structure is built into a linear quadratic synthesis problem to generate state feedback gains. An implementable output feedback solution is found through a linear transformation of the state feedback gain matrix. The control system is gain scheduled with dynamic pressure through polynomial curve fits of linear point design gains. Required maneuvers are demonstrated within design specifications except in cases where the physical limitations of the aircraft restrict achievable performance.**

## Nomenclature

$a_x$ = longitudinal acceleration
$a_y$ = lateral acceleration
$a_z$ = normal acceleration
$p$ = body-axis roll rate
$q$ = body-axis pitch rate
$r$ = body-axis yaw rate
$u$ = velocity with respect to relative wind
$\alpha$ = angle of attack
$\beta$ = sideslip angle
$\gamma$ = flight-path angle
$\delta_A$ = aileron deflection
$\delta_D$ = differential horizontal tail deflection
$\delta_E$ = elevator deflection
$\delta_R$ = rudder deflection
$\delta_{PLA}$ = power level angle
$\phi$ = roll angle

## Introduction

WHILE the area of multivariable control theory has been rapidly advancing over the past 20 years, the application of this theory to actual flying vehicles has lagged behind

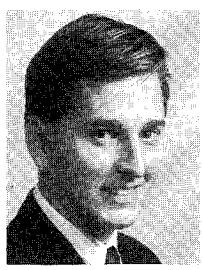

**Richard J. Adams, 1st Lieutenant U.S. Air Force, received a B.S. degree in Engineering Sciences from the United States Air Force Academy in 1989 and an M.S. in Aeronautics and Astronautics from the University of Washington in 1990. He is currently a stability and control engineer in the Flight Dynamics Directorate at Wright Laboratory, Wright-Patterson Air Force Base. His research interests include high angle-of-attack stability and control and the application of multivariable control theory to realistic flight control design. He is a Member of AIAA.**

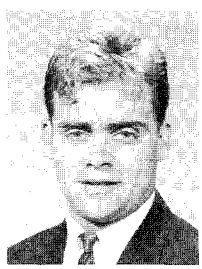

**James M. Buffington is an Aerospace Engineer in the Flight Control Division at Wright Laboratory, Wright-Patterson Air Force Base, Ohio. He studied Aerospace Engineering at the University of Texas at Austin, obtaining a B.S. degree in 1989 and M.S. degree in 1991. His theoretical research interests include optimal control, $H_\infty$ control, fuzzy logic, variable structure control, and direct reduced-order control. Application interests include full envelope flight control, high angle-of-attack flight control, and material process control. He is a Member of AIAA.**

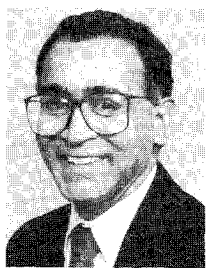

**Dr. Siva S. Banda is an Aerospace Engineer at Wright Laboratory, Wright-Patterson Air Force Base, Ohio. His responsibilities include transitioning basic research results in the area of control theory to the aerospace industry. He has authored or co-authored more than 75 publications in the areas of multivariable control theory and application. He has received numerous awards from the U.S. Air Force for scientific achievement, including the Air Force Chief of Staff award from the Pentagon. He has served as a member of the AIAA Guidance, Navigation, and Control Technical Committee, the Board of Directors of the American Automatic Control Council, Chairman of the AIAA Awards Committee, and Associate Editor of the *Journal of Guidance, Control, and Dynamics.* He has been an Adjunct Associate Professor at Wright State University and at University of Dayton. He is a Fellow of Wright Laboratory and is an Associate Fellow of AIAA.**

Received March 11, 1992; revision received July 30, 1993; accepted for publication July 30, 1993. 

technology. The design of flight controls for operational aircraft is dominated by single-loop approaches using the classical techniques of Bode, Nyquist, Nichols, and root locus. These time-honored methods are well understood and trusted, and produce excellent results for most conventional aerospace configurations operating within conventional environments. As the air vehicle and flight envelope stray from past conventions in the strive for better stealth, performance, or lethality, the advantages of multivariable and robust techniques become evident. The advent of redundant and unconventional control effectors highlights the need for a better way to handle complex multi-input, multi-output (MIMO) systems. As the flight envelope expands into hypersonics and supermaneuverability, the uncertainties that must be tolerated by the modern control systems are increasing. With these increasing demands on the flight control system, the ideas of optimal and robust multivariable control are becoming more popular with both industry and the government. The challenge now is to fill the gap between theory and reality by making the new methods practical for implementation on air vehicles and bridging the confidence gap through successful flight test programs. The need for full-envelope control motivates the implementation issues of linear design theory. Most linear design methods require gain scheduling to make the transition to full-envelope control. Because controllers with a large number of dynamic elements and gains are extremely difficult to gain schedule, the development of low-order multivariable controllers is critical.

A number of flight test programs have used multivariable control synthesis for all or part of their compensator development. In the F-15 STOL maneuvering technology demonstrator program, a linear quadratic gaussian/loop transfer recovery design was used for the nonconventional longitudinal flight control modes.[1] The high-order compensators derived by this method were successfully reduced to a simple PI form. A linear quadratic design was used in the X-31A post stall research aircraft. Multivariable techniques were also used on the advanced fighter technology integration F-16 and F-18 high-alpha research vehicles. All successful flight demonstrations of multivariable control to date have had low-order compensators.

Work has begun on bringing the methods of $H_\infty$ and $\mu$-synthesis into the realm of implementable control design methods. The approach is to pose these designs within a model-following framework that allows for the incorporation of flying quality specifications directly into the design. A recent contracted research effort, robust control law development for modern aerospace vehicles, addressed many of the problems of applying $H_\infty$ control in a model-following approach.[2] The major gap in current technology for this approach is controller order. Work focusing on this problem is ongoing in the Flight Dynamics Directorate.[3]

This paper details the application of one of the earliest and most well-known multivariable design methods, linear quadratic synthesis, to an autopilot design for the AIAA controls design challenge vehicle.[4] The asymptotic properties of linear quadratic regulators (LQRs) are used to incorporate design objectives into the quadratic cost function. A simple linear transformation is made to convert the state feedback LQR result into an implementable output feedback form that retains the desired closed-loop properties.

A nonlinear simulation environment is used to provide simulation control, trimming, and linear model generation for the design challenge vehicle. Linear point design control gains are scheduled using least-squares fit polynomials to provide a wide envelope capability. The control gains are scheduled primarily with dynamic pressure, but also are dependent upon Mach number, altitude, bank angle, and power level angle.

## Background

### Linear Quadratic Design with Integral Action

A linear time-invariant representation of a system in state space form is

$$\dot{x}(t) = Ax(t) + Bu(t), \qquad y(t) = Cx(t) + Du(t) \tag{1}$$

where $t$ is time and $x$, $y$, and $u$ are the state, measurement, and control vector, respectively. For most tracking problems, integral control is desired to achieve zero steady-state error in commanded variables. A design model is formed by augmenting the open-loop plant with integral error states:

$$\dot{x}_a(t) = A_a x_a(t) + B_a u(t), \qquad x_a(t) = [x(t) \int e(t)]^T \tag{2}$$

$$A_a = \begin{bmatrix} A & 0 \\ C_I & 0 \end{bmatrix}, \qquad B_a = \begin{bmatrix} B \\ D_I \end{bmatrix} \tag{3}$$

where $e(t) = r(t) - y_I(t)$ is the tracking error and $y_I(t) = C_I x(t) + D_I u(t)$ is the partition of the output vector $y(t)$ that is commanded by the reference input $r(t)$.

Assuming $D_I = 0$, a quadratic cost function is set up with a control weighting $R$ and a criterion output $y_c(t) = C_c x_a$ that defines a state weighting $Q$:

$$J = \frac{1}{2}\int_0^\infty [x_a^T(t)Qx_a(t) + u^T(t)Ru(t)]\,dt, \qquad Q = C_c^T C_c \tag{4}$$

To take advantage of the asymptotic properties of linear quadratic regulators, the criterion output is chosen to place additional transmission zeros for the controlled outputs:

$$y_c(t) = \sum_{i=1}^{k} [W_{D_i}\dot{e}_i(t) + W_{P_i}e_i(t) + W_{I_i}\int e_i(t)] \tag{5}$$

where $k$ is the number of controlled outputs, and $W_{D_i}$, $W_{P_i}$, and $W_{I_i}$ are the weightings on the derivative, proportional, and integral errors, respectively.[5,6] If this system for control design is minimum phase and has no transmission zeros in the frequency range of interest, the $2k$ additional zeros will attract the integral error states and $k$ additional poles as the control weighting $R$ goes to zero.

The solution is a control history that is a linear function of the state

$$u = -K_x x_a, \quad \text{where} \quad K_x = R^{-1}B_a^T P \tag{6}$$

and $P$ satisfies the algebraic Riccati equation

$$A_a^T P + PA_a - PB_a R^{-1}B_a^T P + Q = 0 \tag{7}$$

This state feedback compensator guarantees stability and robustness properties but may not be implementable due to the lack of full-state measurement. If the number of measured outputs $p$ is greater than or equal to the number of states $n$, and $C$ has full column rank, a transformation is made that retains the eigenvalues of the closed-loop system,

$$K_y = (I - K_x(C^TSC)^{-1}C^TSD)^{-1}K_x(C^TSC)^{-1}C^TS \tag{8}$$

and the control law becomes a linear function of the output

$$u = -K_y y \tag{9}$$

If $p > n$, the output feedback solution is overdetermined and the diagonal matrix $S$ is chosen to adjust the gain on particular feedback signals to reflect practical considerations such as controller decoupling and signal noise. It is important to note that if the output feedback system is not strictly proper, the stability margin guarantees provided by the state feedback solution are no longer valid. In this case, additional robustness analysis is required.

## Full Flight Envelope Design

### Trimming and Linearization

A nonlinear representation of an aircraft has the following form:

$$\dot{x} = f(t, x, u), \quad y = g(t, x, u) \tag{10}$$

where $f$ and $g$ are nonlinear functions. Trimming of the nonlinear system is required to generate linear models at an equi-

librium state and to provide transient free initial conditions for maneuver simulation. A trim solution is found by solving Eq. (10) for the state and control such that specific rates in the left-hand side of the equation are zero. For a conventional fixed-wing aircraft, a trim point is defined by zero acceleration in all six body axes. Once the aircraft is trimmed, a linear representation of the aircraft is obtained using perturbation techniques. The resulting linear model represents vehicle dynamics within a region around the equilibrium condition,

$$\dot{x}(t) = Ax(t) + Bu(t), \quad y(t) = Cx(t) + Du(t) \tag{11}$$

**Open-Loop Analysis**

Singular value analysis of the open-loop plant models shows that standard partitioning of the plant into separate longitudinal and lateral/directional systems is practical for analysis and design. Eigenstructure analysis shows that the lateral/directional behavior of the vehicle is stable and very well behaved for all design conditions. An increase in dutch-roll damping and a decrease in the roll mode time constant is desirable for a fast, decoupled lateral/directional response. The longitudinal dynamics exhibit classical short period and phugoid modes that are relatively stable throughout the envelope. The benevolent behavior of the open-loop system allows for simple stability augmentation and focuses the design on the trajectory following autopilot.

**Control Structure**

The longitudinal and lateral/directional control systems have similar structures. Figure 1 is a block diagram of the entire aircraft control system. The longitudinal axis is controlled by an output feedback regulator that tracks Mach number and flight path angle and augments vehicle stability. Two transformations are performed in the longitudinal control system. The transformation $T1$, a function of velocity with respect to the relative wind, generates a flight path angle command from the altitude rate command. The transformation $T2$, a function of the speed of sound, generates a Mach signal from the velocity output. The altitude rate command input is integrated to form an altitude position command signal. The other input is Mach number command, which is rate-limited to reduce the buildup of errors. The lateral/directional axes are controlled by an output feedback regulator that tracks bank angle and provides aircraft state stabilization. A constant lag prefilter is used in the bank angle command path to generate the desired first-order roll response. For maneuvers that generate cross-axis coupling, a cross-axis filter generates a longitudinal command increment from a bank angle input.

**Longitudinal Design**

The longitudinal design model contains integral velocity and flight path angle error states. The state vector is

$$x_{\text{long}} = [u_{\text{err}} \alpha q \gamma_{\text{err}} \delta_E \delta_{\text{PLA}} \int u_{\text{err}} \int \gamma_{\text{err}}]^T \tag{12}$$

the inputs are

$$u_{\text{long}} = [\delta_E \delta_{\text{PLA}}] \tag{13}$$

and the outputs are

$$y_{\text{long}} = [u_{\text{err}} \alpha q \gamma_{\text{err}} \int u_{\text{err}} \int \gamma_{\text{err}} a_z a_x]^T \tag{14}$$

The longitudinal actuator dynamics are too slow to be separated from the control bandwidth and thus are included in the design model.

The elevator dynamics are represented by a first-order lag with a time constant of 0.05 s. The engine dynamics are approximated as a first-order lag with a flight condition-dependent time constant and gain. To avoid the need for a more complicated gain schedule, a constant time constant is chosen as the design value and the variation across the envelope is treated as unstructured uncertainty. The engine gain is the local slope of the thrust vs the power level angle curve and thus is a function of Mach, altitude, and power level angle (PLA). To remove the flight condition dependency of this gain, a constant value is assumed for design and the actual variation is accounted for by normalizing the thrust effectiveness in the nonlinear implementation.

The targeted velocity and flight path angle responses are contained in the state weighting matrix. Proportional, integral, and derivative velocity and flight path angle tracking errors are included in the cost function. The elevator and power level angle positions are weighted within the control

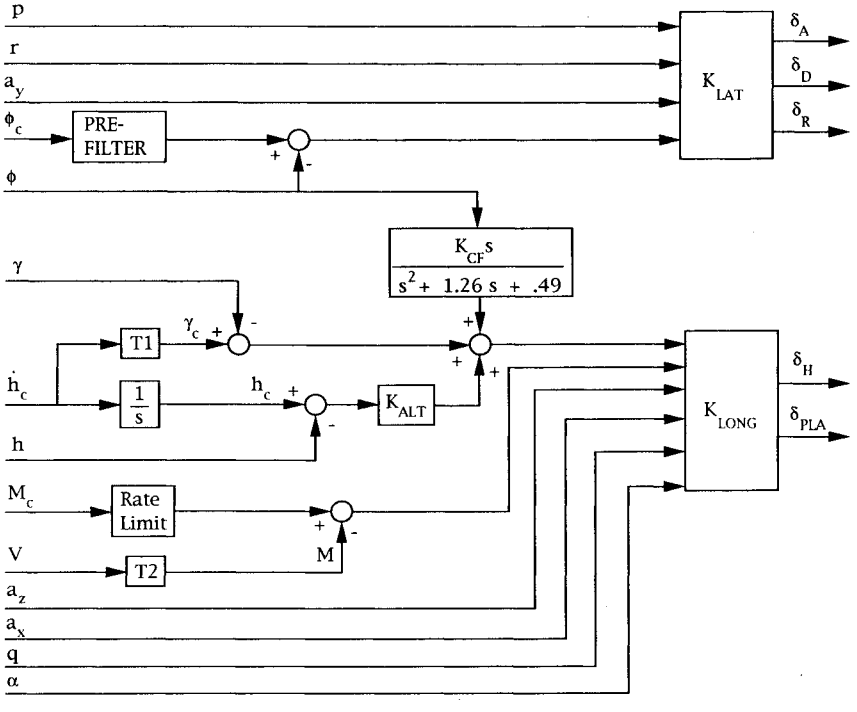


**Fig. 1 Controller structure.**

weighting matrix. After the output feedback gains are computed, the longitudinal control system is decoupled by deleting velocity error feedbacks to the elevator and removing all feedback paths to power level angle except the PID velocity errors. This prevents undesirable control interactions that occur because the engine responds significantly slower than the elevator. The altitude feedback path is designed classically as an outer loop wrapped around the linear quadratic design. This loop provides good low-frequency tracking of altitude.

#### Lateral/Directional Design

The lateral/directional design model contains an integral bank angle error state. The state vector is

$$x_{\text{lat/dir}} = [\beta pr\phi_{\text{err}}\textstyle\int\phi_{\text{err}}]^T \tag{15}$$

the inputs are

$$u_{\text{lat/dir}} = [\delta_A \delta_D \delta_R] \tag{16}$$

and the outputs are

$$y_{\text{lat/dir}} = [a_y pr\phi_{\text{err}}\textstyle\int\phi_{\text{err}}]^T \tag{17}$$

The lateral/directional actuator states are not included in the design model. It is possible to maintain sufficient separation between the control bandwidth and the actuator dynamics to prevent significant degrading of stability margins.

The targeted bank angle response is embedded in the design structure within the state weighting matrix. Proportional, integral, and derivative bank angle tracking errors are included in the cost function. Sideslip magnitude is also included in the cost to reduce the buildup of sideslip during banking maneuvers. The aileron, differential horizontal tail, and rudder deflections are weighted in the control weighting matrix. The feedback of roll rate to the rudder is removed because of negligible gain on that signal.

The cross-axis controller is a second-order filter with a derivative output. The filter responds to bank angle input by producing a transient command to the longitudinal controller. It is designed within the nonlinear environment to minimize errors in altitude and Mach number during turning maneuvers.

#### Nonlinear Implementation

A gain schedule provides full envelope integration of the control system. Point designs are integrated through least-squares polynomial curve fits in dynamic pressure. Because there are only four prescribed flight conditions, nine other design conditions, six subsonic and three supersonic, are selected to obtain an accurate gain schedule. Figure 2 is used to select the design conditions by obtaining a complete cross section of dynamic pressures across the flight envelope.

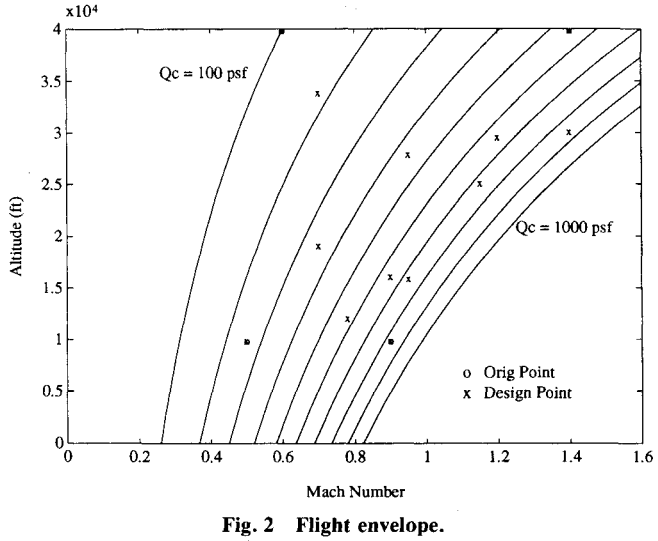


**Fig. 2 Flight envelope.**

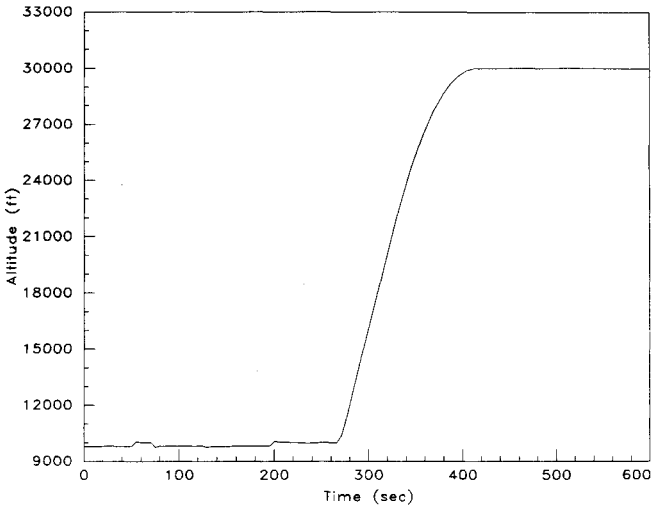


**Fig. 3 Composite maneuver altitude response.**

The linearly designed elevator, aileron, differential horizontal tail, and rudder gains are used to fit the lowest feasible order polynomial in dynamic pressure with a linear least-squares data-fitting technique.[7] The elevator gains are split into subsonic gains and supersonic gain increments. The supersonic increments are blended with the subsonic gains as the aircraft transitions between subsonic and supersonic flight.

In the linear design phase, a constant value is assumed for the engine dynamics model gain. This gain is actually the slope of the thrust vs the power level angle curve and it varies significantly with flight condition. To implement the power level angle feedback paths, compensation is made for the actual changing thrust effectiveness by normalizing the engine thrust response. This normalization is achieved by multiplying the power level angle feedback signals by the design value of engine gain divided by an estimated engine effectiveness. This estimate of engine effectiveness is a function of Mach number, altitude, and power level angle.

The altitude gain is scheduled against bank angle and Mach number. The cross-axis filter gain is scheduled against bank angle, Mach number, and dynamic pressure.

Control effector saturation is another problem that is addressed in the nonlinear implementation of control laws. When an effector saturates, it creates a situation in which it is impossible to track the commanded variables. In a linear sense, one of the integrators in the controller becomes unstabilizable. This condition creates undesirable trends in the control histories during nonlinear simulation. A solution is to close a local feedback loop around the unstabilizable integrator, making the overall system stable. A local loop is closed around the flight path angle error integrator if the elevator saturates and around the velocity error integrator if the power level angle saturates. Lateral/directional control saturation is not a problem in this design.

## Results And Analysis

Recall that the prescribed design maneuvers are the following: 2-$g$ turn, 3-$g$ turn, 50-ft/s climb, and level acceleration from a subsonic to a supersonic condition. All maneuvers must hold altitude within $\pm 50$ ft and Mach number within $\pm 0.01$ of commanded values. During climbs and the acceleration, the aircraft must maintain a zero sideslip angle $\pm 1.0$ deg and zero roll angle $\pm 5.0$ deg. For constant $g$ turns, the aircraft must maintain a zero sideslip angle $\pm 2.0$ deg and a load factor within $\pm 0.2$ $g$ of the commanded value. The ability of the fighter to perform the required maneuvers is limited by control effector rate limits and available control power. All design requirements defined by the Guidance, Navigation, and Con-

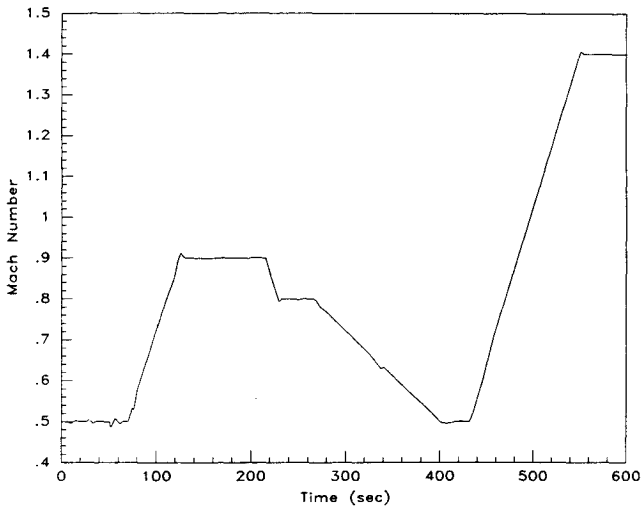


**Fig. 4 Composite maneuver Mach number response.**

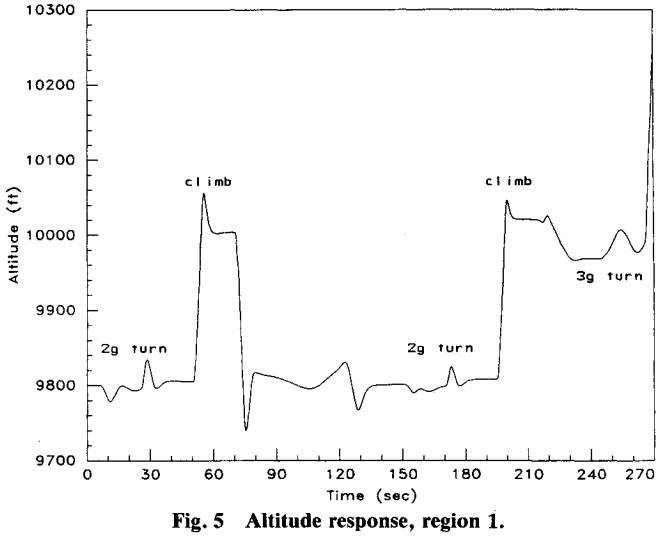


**Fig. 5 Altitude response, region 1.**

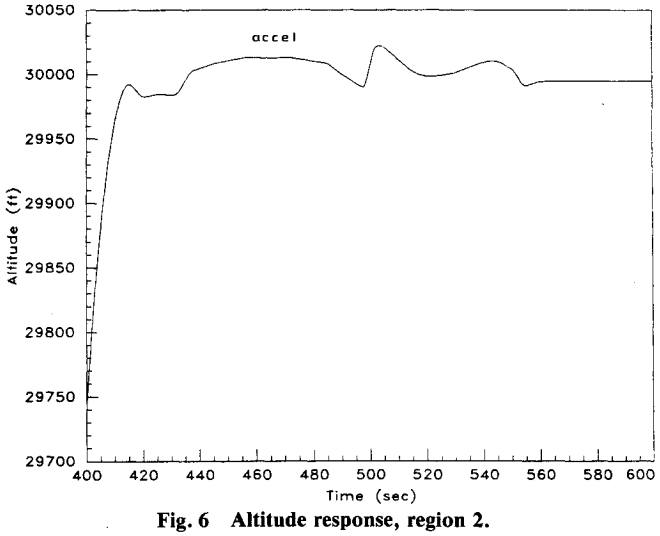


**Fig. 6 Altitude response, region 2.**

trol Technical Committee are satisfied for the maneuvers that take place at $M = 0.9$, $h = 9800$ ft and $M = 1.4$, $h = 39{,}800$ ft. For $M = 0.5$, $h = 9800$ ft, the 2-$g$ turn requirements are met, but in the climb maneuver, the altitude specification is violated by 6.5 ft and the Mach specification is violated by 0.004. The violation of the altitude specification is caused by the limited angular rates available for the horizontal tail. For $M = 0.6$, $h = 39{,}800$ ft, open loop trim analysis shows that a sustained 2-$g$ turn is impossible due to insufficient control power. Rate saturation of the elevator limits the achievable climb performance; the maneuver is achieved with large transient errors in altitude and Mach number.

For most flight conditions that require an afterburner to hold Mach number, the discrete augmenter rings that are represented in the thrust model make it impossible to achieve a steady-state trim solution. A limited number of augmented thrust levels are available at any specific flight condition. Since the closed-loop controller uses throttle setting to hold airspeed, limit cycling occurs as the power level angle is adjusted to find a trim setting that does not exist. One solution

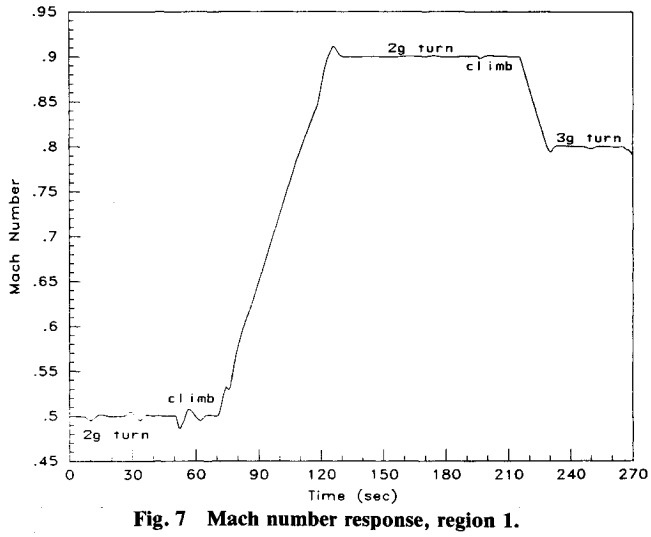


**Fig. 7 Mach number response, region 1.**

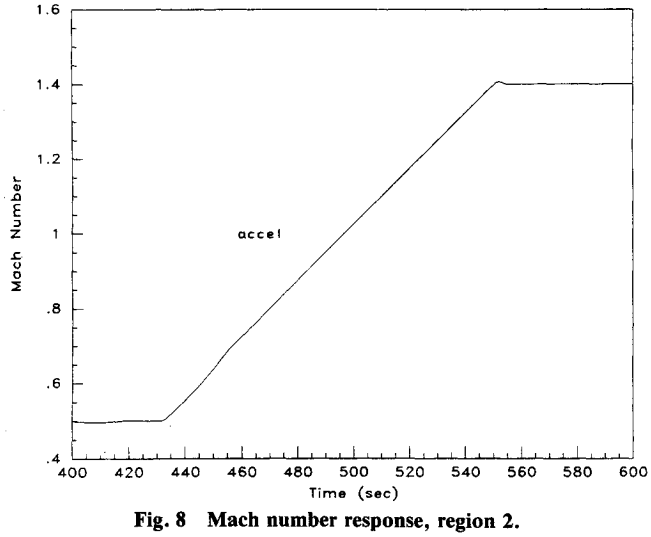


**Fig. 8 Mach number response, region 2.**

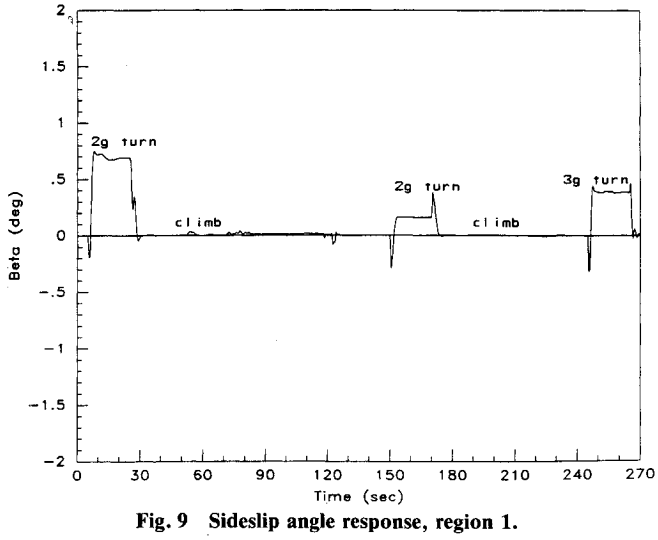


**Fig. 9 Sideslip angle response, region 1.**

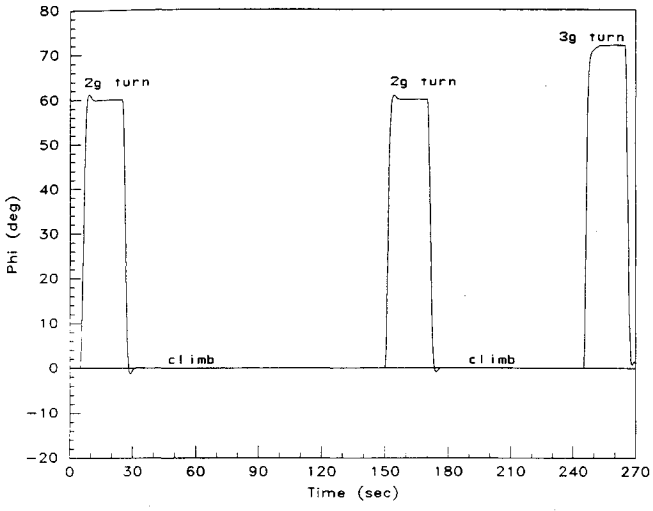


**Fig. 10 Roll angle response, region 1.**

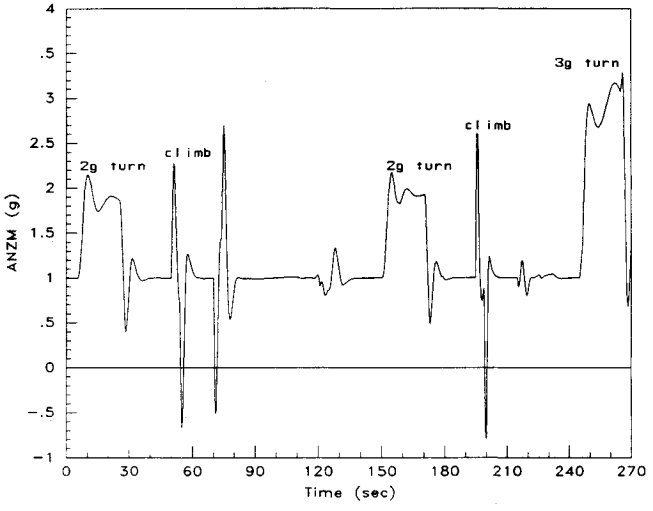


**Fig. 11 Normal acceleration response, region 1.**

to this problem is to put a deadband in the Mach error path to represent an error tolerance. This approach is not feasible for the AIAA aircraft because the thrust differential between each ring is too large. More investigation into control solutions for the trim and limit cycling problems has not been conducted because of concerns about the fidelity of the engine dynamics model. If variable pressure rings, which are common on modern fighter aircraft, were represented in the nonlinear model, the magnitude of this problem would be reduced considerably.

A composite maneuver is simulated to demonstrate performance across the design envelope. The simulation run consists of six design maneuvers and various others to transition between design conditions. The first and second maneuvers are a 2-$g$ turn and 50-ft/s climb at $M = 0.5$, $h = 9800$. The third and fourth maneuvers demonstrate turn and climb performance at $M = 0.9$, $h = 9800$. The last two maneuvers are the 3-$g$ turn and the climb from Mach 0.5 to 1.4 level acceleration. The Mach, altitude, load factor, roll angle, and sideslip specifications are satisfied for these two maneuvers. Table 1 gives an outline of the composite maneuver. Figures 3 and 4 show time responses of altitude and Mach number for the entire

**Table 1 Composite maneuver**

| Time, s | Mach Number | Altitude, Kft | Maneuver | Maneuver Type |
|---|---|---|---|---|
| 0–25 | 0.5 | 9.8 | 2-$g$ turn | Design |
| 25–54 | 0.5 | 9.8–10 | 50-ft/s climb | Design |
| 54–150 | 0.5–0.9 | 10–9.8 | Accel/dive | Transfer |
| 150–195 | 0.9 | 9.8 | 2-$g$ turn | Design |
| 195–215 | 0.9 | 9.8–10 | 50-ft/s climb | Design |
| 215–245 | 0.9–0.8 | 10 | Decel | Transfer |
| 245–265 | 0.8 | 10 | 3-$g$ turn | Design |
| 265–430 | 0.8–0.5 | 10–30 | Decel/climb | Transfer |
| 430–600 | 0.5–1.4 | 30 | Accel | Design |

maneuver. Figures 5–11 show time responses of the critical flight parameters with the transition region from 270 to 400 s excluded because it is a smooth climb/deceleration that does not include any required maneuvers.

Stability margins are calculated for individual loops broken at the inputs to the actuators and the outputs of the sensors. The resulting gain and phase margins represent the level of signal deterioration/uncertainty that can be tolerated before the closed-loop system becomes unstable. The margins for the actuator and sensor loops reflect satisfactory robustness for reasonable levels of gain and phase perturbations at a wide range of flight conditions.

## Conclusions

One possible solution to the AIAA controls design challenge is presented. The underlying advantages of this proportional plus integral plus derivative design are simplicity and implementability. Mach number and altitude tracking and level turning performance have been achieved within the physical limitations of the aircraft. The rate limit on horizontal tail actuation is the greatest single constraint on performance. A composite maneuver demonstrates that the implemented control laws provide continuous regulation and tracking across the flight envelope.

## References

[1]Moorhouse, D. J., and Kisslinger, R. L., "Lessons Learned in the Development of a Multivariable Control System," *Proceedings of the National Aerospace and Electronics Conference* (Dayton, OH), Inst. of Electrical and Electronics Engineers Service Center, Piscataway, NJ, 1989, pp. 364–371.

[2]Chiang, R. Y., Safonov, M. G., Haiges, K. R., Madden, K. P., and Tekawy, J. A., "A Fixed $H_\infty$ Controller for a Supermaneuverable Fighter Performing a Herbst Maneuver," *Automatica,* Vol. 29, No. 1, 1993, pp. 111–127.

[3]Yeh, H. H., Rawson, J. L., and Banda, S. S., "Robust Control Design with Real-Parameter Uncertainties," *Proceedings of the American Control Conference* (Chicago, IL), Inst. of Electrical and Electronics Engineers Service Center, Piscataway, NJ, 1992, pp. 3249–3254.

[4]Brumbaugh, R. W., "An Aircraft Model for the AIAA Controls Design Challenge," AIAA Paper 91-2631, Aug. 1991.

[5]Harvey, C. A., and Stein, G., "Quadratic Weights for Asymptotic Regulator Properties," *IEEE Transactions on Automatic Control,* Vol. AC-23, No. 3, 1978, pp. 378–387.

[6]Thompson, C. M., Coleman, E. E., and Blight, J. D., "Integral LQG Controller Design for a Fighter Aircraft," *Proceedings of the AIAA Guidance, Navigation, and Control Conference* (Monterey, CA), AIAA, Washington, DC, 1987, pp. 866–895 (AIAA Paper 87-2452).

[7]Golub, G. H., and Van Loan, C. F., *Matrix Computations,* The Johns Hopkins Univ. Press, Baltimore, MD, 1989, Chap. 5, pp. 221–253.